Unilateral regulation breaks regularity of Turing patterns

Tomáš Vejchodský

Filip Jaroš

Milan Kučera

Vojtěch Rybář

UNILATERAL REGULATION BREAKS REGULARITY OF TURING PATTERNS

TOMÁŠ VEJCHODSKÝ, FILIP JAROŠ, MILAN KUČERA, VOJTĚCH RYBÁŘ

ABSTRACT. We consider a classical reaction-diffusion system undergoing Turing instability and augment it by an additional unilateral source term. We investigate its influence on the Turing instability and on the character of resulting patterns. The nonsmooth positively homogeneous unilateral term τv^- has favourable properties in spite of the fact that the standard linear stability analysis cannot be performed. We illustrate the importance of the nonsmoothness by a numerical case study, which shows that the Turing instability can considerably change if we replace this term by its arbitrarily precise smooth approximation. However, the nonsmooth unilateral term and all its approximations yield qualitatively same patterns although not necessarily developing from arbitrarily small disturbances of the spatially homogeneous steady state. Further, we show that inserting the unilateral source into a classical system breaks the approximate symmetry and regularity of the classical patterns and yields asymmetric and irregular patterns. Moreover, a given system with a unilateral source produces spatial patterns even for diffusion parameters with ratios closer to 1 than the same system without any unilateral term. Biologically, these findings can contribute to the understanding of symmetry breaking during morphogenesis.

1. INTRODUCTION

Reaction-diffusion systems are frequently used to model the initiation of animal forms and patterns. After publication of Turing's purely theoretical paper [26], growing number of biologists succeeded in matching empirical data with mathematical simulations. Morphogens with Turing-like behaviour were found in the process of hair follicles formation [20], the generation of transverse ridges of the palate [6] or patterning the germ layers [2, 24]. The concept of reactions and diffusion of morphogens was widened to the interactions of pigment cells. In

1

the case of zebrafish, the validity of this model was tested on individuals with ablated skin [15, 16]. Turing's mechanism is also used to model the formation of coat patterns in mammals, see for example [19, 21].

We will consider reaction-diffusion systems of the type

$$\frac{\partial u}{\partial t} = d_1 \Delta u + f(u,v) \quad \text{in } \Omega, \tag{1}$$

$$\frac{\partial v}{\partial t} = d_2 \Delta v + g(u,v) + \hat{g}(v) \quad \text{in } \Omega$$

with the usual homogeneous Neumann boundary conditions

$$\frac{\partial u}{\partial n} = \frac{\partial v}{\partial n} = 0 \quad \text{on } \partial\Omega. \tag{2}$$

The domain $\Omega \subset \mathbb{R}^2$ represents the tissue, t denotes the time variable, $u = u(x,y,t)$ and $v = v(x,y,t)$ stand for concentrations of two morphogens, d_1 and d_2 are their diffusion coefficients and smooth functions $f(u,v)$ and $g(u,v)$ describe kinetics of the system given by interactions between the morphogens, n stands for the unit outward facing normal vector to the boundary $\partial\Omega$. A novelty is an additional term $\hat{g}(v)$ which is unilateral in the sense that there exists a threshold value θ such that $\hat{g}(v) > 0$ for $v < \theta$ and $\hat{g}(v) = 0$ otherwise. This term describes an additional source active only if the concentration of the second morphogen decreases below the threshold θ. The key point is that the function $\hat{g}(v)$ can be nonsmooth, a typical example being $\hat{g}(v) = \tau(v - \theta)^-$, where $(v - \theta)^- = (|v - \theta| - v + \theta)/2$ stands for the negative part of $v - \theta$ and $\tau > 0$ controls the strength of this unilateral source. Our goal will be to investigate the influence of the unilateral term $\hat{g}(v)$ to the Turing instability and to the formation of spatial patterns (spatially nonconstant stationary solutions). From these points of view we will compare the unilateral and classical systems, i.e. system (1) with a unilateral term $\hat{g}(v)$ and the corresponding classical system with $\hat{g} \equiv 0$.

Let $\bar{u}$ and $\bar{v}$ be such constants that $f(\bar{u}, \bar{v}) = g(\bar{u}, \bar{v}) + \hat{g}(\bar{v}) = 0$. Consequently, $u = \bar{u}$, $v = \bar{v}$ is a spatially constant stationary solution to (1) with (2). We refer to this constant steady state as a *ground state*. The *Turing diffusion driven instability* is characterized by the stability of the ground state with respect to small spatially *homogeneous* perturbations and its instability with respect to small spatially *nonhomogeneous* perturbations.

In the classical (smooth) case, we can perform the well known linear analysis, to find necessary conditions for the Turing instability to occur, see e.g. [7, 12, 21]. If these conditions are satisfied then starting from small nonhomogeneous disturbances of the ground state, the solution of (1) can converge to another, spatially nonhomogeneous steady state, provided it exists. In biology, this process of forming nonhomogeneous steady states can serve as a model of pattern (prepatern) formation mechanisms. Therefore, we often refer to these spatially nonhomogeneous stationary solutions as patterns. We will have $\partial f/\partial u(\bar{u}, \bar{v}) > 0$ in systems under consideration and we will call u the activator and v the inhibitor. In this

case, one of the necessary conditions for the Turing instability is that the diffusion coefficient of the activator is sufficiently smaller than the diffusion coefficient of the inhibitor, i.e. the ratio d_1/d_2 is sufficiently small.

Our paper is motivated mainly by two surprising results [17] and [14] about systems, where the unilateral term is not given by $\hat{g}$ as in (1), but by certain unilateral conditions for v formulated by variational inequalities. The former result guarantees existence of stationary spatially nonhomogeneous solutions even for d_1/d_2 arbitrarily large. The later result concerns certain instability of the ground state for a wide range of values d_1 and d_2 including arbitrary size of the ratio d_1/d_2. There are also theoretical studies, e.g. [5, 8, 9, 10, 18] and references therein, predicting new and interesting features of systems with various unilateral terms or conditions.

The unilateral conditions described by variational inequalities considered in [14, 17] correspond to sources which do not allow the concentration of the morphogen v to decrease below a threshold θ on a given subset of the boundary or of the interior of the domain. These hard inequalities, however, seem to be unrealistic from the viewpoint of biological applications, because it is difficult to imagine a natural mechanism which would strictly prevent the concentration of a morphogen to decrease below the threshold.

Therefore, we consider a unilateral term $\hat{g}(v)$ in (1). This term corresponds to a source, which is active only in those places, where the concentration v is below the value θ. It does not prevent the concentration of v to decrease below θ, but it works against this decrease. Our goal is to investigate this case and find for what values of the ratio d_1/d_2 the Turing instability occurs, what is the kind of the resulting patterns and what biological implications it can have. These questions have not been addressed before and we aim to answer them in this paper.

We will consider simple choices of the nonsmooth unilateral term, mainly $\hat{g}(v) = \tau(v - \theta)^-$ and its approximations. Unilateral terms of this type have been introduced in the context of reaction-diffusion systems exhibiting the Turing instability already in [9]. However, the stability of the ground state with respect to small spatially homogeneous perturbations as well as its instability with respect to small spatially nonhomogeneous perturbations has not been analysed for this type of systems. This analysis is nontrivial, because the possible nonsmoothness of the unilateral term precludes the use of the standard linear analysis. Moreover, we show in Section 3 below that the ground state in systems with the nonsmooth unilateral term is stable under different conditions than in systems with smooth approximations of this nonsmooth unilateral term. On the other hand, we also show that perturbations of not necessarily arbitrary small size do evolve to qualitatively same patterns under the same conditions for both the nonsmooth unilateral term and its smooth approximations. Thus, the fact whether an arbitrarily small perturbation of the ground state will evolve to a pattern or not is extremely sensitive to small changes of the nonlinear dynamics

near the ground state. A small change of the nonlinear dynamics in the neighbourhood of the ground state can turn a stable system to the unstable and vice versa. However, the numerical case study we performed indicates that if the initial perturbations of the ground state are larger than a certain minimal size then they robustly evolve to qualitatively same patterns regardless small changes of the nonlinear dynamics near the ground state.

Theoretically, it is not clear how to analyse the evolution of perturbations of the ground state that are larger than a certain minimal size. Such theory does not exist. However, the nonsmoothness of the unilateral term could help. We observe, at least in the particular examples presented below, that in cases when smooth approximations yield patterns for larger perturbations only, the nonsmooth term yields qualitatively same patterns even from arbitrarily small perturbations. Thus, the question whether the larger perturbations of the ground state will evolve to patterns in systems with (both smooth and nonsmooth) unilateral term or not seems to correspond to the question of stability with respect to arbitrarily small perturbations of the system with the nonsmooth unilateral term. Theoretical study of the question what are the parameters for which spatially nonhomogeneous stationary solutions exist is done in [9] for the case of nonsmooth terms of the type τv^-, not for their smooth approximations. Further theoretical results about various other (nonsmooth) unilateral conditions can be found in above mentioned papers. These possibilities of new theoretical approaches further motivate our interest in nonsmooth unilateral terms even if their smooth approximation can perhaps seem to be more natural from the point of view of applications.

Here, we do not attempt to analyse system (1) in its full generality due to the complexity of this task. Instead, we present a case study of a reaction-diffusion system from [1, 19] appended by a unilateral term.

The rest of this paper is organized as follows. Section 2 explains possible biological mechanisms that can be modelled by the unilateral source terms and motivates the choice $\theta = \bar{v}$. Section 3 shows the significance of the nonsmooth unilateral term $\hat{g}(v) = \tau(v - \bar{v})^-$ and compares its influence on the initiation and final formation of spatial patterns with the influence of its approximations. Section 4 presents numerical experiments showing spatial patterns produced by a unilateral system (1), compares them with patterns obtained by the classical system without any unilateral term, and shows how these patterns depend on the strength of the unilateral source and on the ratio of diffusion constants. In general, we observe that unilateral terms yield asymmetric patterns with irregular spots. In addition, for the studied choice of f and g, the system (1) with a unilateral term $\hat{g}(v)$ generates patterns even for greater ratio of diffusions in comparison with the classical system. Finally, we show that the difference between the patterns corresponding to the almost zero and high strength of the unilateral source resembles the difference between the roughly regular pattern of the wild

type cheetah and the irregular pattern of the king cheetah. Section 5 discusses the results and draws the conclusions.

2. Biological motivation of unilateral sources

System (1) models diffusion and interactions of two morphogens within a tissue. These interactions can include direct chemical reactions between the two morphogens and also highly nontrivial interactions mediated by the presented cells. These nontrivial interactions can be modelled by the classical nonlinear terms f and g in system (1), but they can also account for the action of the unilateral source $\hat{g}$. For example, we may consider the unilateral term $\hat{g}(v) = \tau(v - \theta)^-$ or similar (for example its smooth approximation). Receptors in the cell membrane can detect the local concentration of the morphogen v. If this concentration decreases below the threshold value θ, the receptors initiate a signalling pathway that results to the production of the morphogen v by the cell. The lower the concentration of v decreases below the threshold the higher is the production of the morphogen. Once the concentration of the morphogen increases above the threshold value θ, the receptors stop the signalling and the production of the morphogen terminates. This process is well described by the term $\hat{g}(v) = \tau(v - \theta)^-$. Indeed, in points $(x, y) \in \Omega$ and times t, where $v(x, y, t) < \theta$, the term $\tau(v(x, y, t) - \theta)^-$ is positive and works as a source term in (1). On the other hand, in points $(x, y) \in \Omega$ and times t, where $v(x, y, t) \geq \theta$, the term $\tau(v(x, y, t) - \theta)^-$ vanishes and has no effect.

When ontogeny of an organism is considered, the natural value for the threshold seems to be around the ground state, i.e. $\theta \approx \bar{v}$. Indeed, we may provide the following simplistic, but biologically plausible explanation. In the early stages of the ontogeny, the organism is small. Hence, the size of the domain Ω is not sufficient for spatially nonhomogeneous solutions to form and the only stable solution to (1) is the ground state $\bar{u}, \bar{v}$. Thus, it is natural to assume that the concentrations settle close to this steady state and stay there for a considerable amount of time. For this reason the tissue may consider this value as a normal and satisfactory state. However, as the tissue grows, the diffusion driven instability occurs and the concentrations start to diverge from the levels $\bar{u}, \bar{v}$. According to the principle of homeostasis [11], the tissue may try to balance the concentrations back by reacting as described above. Therefore, it is natural to consider the threshold $\theta \approx \bar{v}$.

In this paper, we will consider the threshold mostly at the ground state, i.e. $\theta = \bar{v}$. However, it is demonstrated in Section 3 that threshold values chosen slightly above or below $\bar{v}$ yield qualitatively the same patterns. The difference is that these patterns need not arise from arbitrarily small disturbances, but only from those having a certain minimal size corresponding to the distance $\bar{v} - \theta$. However, if this distance is very small then it makes no difference from the biological point of view.

Let us note that the above simplified explanation ignores the grows of the organism during ontogeny. Although it is well known that the grows of the domain Ω has fundamental consequences for the pattern formation, see e.g. [4, 3, 27], the basic idea described above is valid, because even the models with growing domains exhibit no spatial patterns if the domain is small.

Concerning the shape of function $\hat{g}$, we will mainly use a simple choice $\hat{g}(v) = \tau(v-\theta)^-$ and its various approximations in this paper. However, in order to model the biologically relevant features accurately, we can modulate the function $\hat{g}$ to control the performance and the strength of the unilateral source. For example, we could set $\hat{g}(v) = \tau(1 - \exp[-(v-\theta)^-])$ to models the limited ability of cells to produce the morphogen. The lower is the concentration v below θ, the higher is the production of v, but the rate of production quickly saturates at the value τ, because, clearly, $\tau(1 - \exp[-(v-\theta)^-]) \to \tau$ as $v \to -\infty$.

3. Significance of the nonsmooth unilateral term

As we have already mentioned, the unilateral term need not be smooth at the point of the ground state and, therefore, the standard linear analysis cannot be performed, in general. If the unilateral term is non-smooth at the ground state, a natural idea is to approximate it by a smooth one. Such approximation can be arbitrarily precise and therefore we would expect that the behaviour of the approximate system will not considerably differ from the behaviour of that with the nonsmooth unilateral term. This vague statement is roughly correct from the perspective of the formation of the final pattern, but it is not true from the point of view of the Turing instability. The reason is that the Turing instability is a local effect determined by small perturbations of the ground state, but the shape of the final pattern is formed by nonlinear terms f, g, and $\hat{g}$ evaluated at points u and v distant from the ground state. To illustrate this phenomenon, we provide a short case study to show how various approximations of the unilateral term may influence the Turing instability and what are their effects on the resulting patterns. Basically, we show that the occurrence of the Turing instability is extremely sensitive on small changes of the nonlinear dynamics near the ground state.

We will discuss the particular system used in [1, 19] for the study of skin and coat patterns in fish and mammals, and supplement it by a unilateral source term $\hat{g}(v)$. Namely, we will consider the system

$$\frac{\mathrm{d}u}{\mathrm{d}t} = D\delta\Delta u + \alpha u + v - r_2 uv - \alpha r_3 uv^2 \quad \text{in } \Omega, \tag{3}$$

$$\frac{\mathrm{d}v}{\mathrm{d}t} = \delta\Delta v - \alpha u + \beta v + r_2 uv + \alpha r_3 uv^2 + \hat{g}(v) \quad \text{in } \Omega.$$

Note that this system is a special case of (1) with $d_1 = D\delta$, $d_2 = \delta$, $f(u,v) = \alpha u + v - r_2 uv - \alpha r_3 uv^2$, and $g(u,v) = -\alpha u + \beta v + r_2 uv + \alpha r_3 uv^2$. Further note that the original system in [1, 19] is formulated in such a way that the original

real positive ground state is shifted to zero. This means that u and v in (3) do not denote concentrations as in Section 1, but their deviations from their original ground state, see [1]. Nevertheless, this difference is unimportant. As in [19], we will assume the homogeneous Neumann boundary conditions (2) and parameter values

$$\delta = 6, \ \alpha = 0.899, \ \beta = -0.91, \ r_2 = 2, \ r_3 = 3.5. \tag{4}$$

For D we will consider several different values.

The ground state of system (3) is defined in the same way as in Section 1, i.e. it consists of constants $\bar{u}, \bar{v}$ such that $f(\bar{u}, \bar{v}) = g(\bar{u}, \bar{v}) + \hat{g}(\bar{v}) = 0$. Clearly, $\bar{u} = \bar{v} = 0$ for those $\hat{g}$ satisfying $\hat{g}(0) = 0$. This is the case for choices of $\hat{g}$ we are mainly interested in. However, certain choices of $\hat{g}$ introduced below do not vanish at zero and hence the corresponding ground state is nonzero.

In the case when the additional unilateral term $\hat{g}(v)$ in (3) is smooth at $\bar{v}$, we can perform the standard linear analysis to obtain necessary conditions for the Turing instability, see e.g. [7, 12, 21]. Namely, we can introduce the Jacobi matrix of the map f, $g + \hat{g}$ at $\bar{u}, \bar{v}$ as

$$B = \left[\begin{array}{cc} b_{11}, & b_{12} \\ b_{21}, & b_{22} \end{array} \right] = \left[\begin{array}{cc} \partial f/\partial u, & \partial f/\partial v \\ \partial g/\partial u, & \partial g/\partial v + \partial \hat{g}/\partial v \end{array} \right] (\bar{u}, \bar{v}). \tag{5}$$

If

$$\operatorname{tr} B < 0 \quad \text{and} \quad \det B > 0, \tag{6}$$

then the ground state $(\bar{u}, \bar{v})$ is stable with respect to small spatially homogeneous perturbations. If simultaneously

$$b_{11}b_{22} < 0 \text{ and } b_{12}b_{21} < 0 \tag{7}$$

then this ground state is stable (with respect to small spatially nonhomogeneous perturbations) only for some values of D and unstable for others, see e.g. [21, sec. 2.3].

Parameter values (4) are chosen in such a way that for $\hat{g} \equiv 0$ conditions (6) and (7) are fulfilled. In any case, if $\hat{g}(v)$ is smooth at $\bar{v}$ and if conditions (6) and (7) hold then a necessary condition for the ground state of system (3) to be unstable with respect to spatially nonhomogeneous perturbations is that the ratio of diffusion coefficients D is sufficiently small. Precisely, the condition is

$$D < D_{\mathrm{crit}} \quad \text{with} \quad D_{\mathrm{crit}} = \frac{1}{b_{22}^2} \left(\det B - b_{12}b_{21} - 2\sqrt{-b_{12}b_{21} \det B} \right). \tag{8}$$

Note that the definition of D_{crit} in (8) is just a reciprocal value of the formula from [22, p. 562]. It can also be easily derived from the analysis of [21, p. 109]. In any case, if condition (8) is not satisfied then the Turing instability cannot occur. It is essential that if $\hat{g}$ is not smooth at the ground state value $\bar{v}$ then this linear analysis cannot be performed. Jacobian B is simply not defined and consequently formula (8) has no sense. Regions of D for which the trivial solution is stable

or unstable, i.e. the critical border D_{crit} between stability and instability, can be only estimated numerically.

The following Subsection 3.1 defines six different choices of $\hat{g}(v)$ and compares them with respect to the Turing instability. We emphasize that the Turing instability is a local phenomenon determined by *arbitrarily small* perturbations and hence only the values of $\hat{g}(v)$ in a small neighbourhood of the ground state $\bar{v}$ are relevant. We will see that although the six choices of $\hat{g}(v)$ differ only slightly in the neighbourhood of the ground state, some of them yield patterns evolving from arbitrarily small perturbations and some of them do not. However, further in Subsection 3.2 we will see that if the perturbations of the ground state are *larger* than a certain minimal size, then they evolve to qualitatively same patterns in all cases.

We note that all systems in this paper are solved numerically by our own finite element solver. For the initial condition we always choose small random fluctuations around the ground state, except of Figure 3, where the fluctuations are larger. Clearly, different initial conditions may and often do evolve to different stationary solutions, but qualitative features of these solutions are the same. We choose the domain to be $\Omega = (-100, 100)^2$ and in the subsequent figures, we plot the patterns as graphs of the solution component u, where values of u are indicated by shades of grey. We do not plot the component v, because it is complementary to u, see [21, p. 88], and patterns based on v are almost identical to patterns based on u.

3.1. **Turing instability for various choices of $\hat{g}(v)$.** Now, we will consider different choices of $\hat{g}(v)$ and compare their influence on the Turing instability, i.e. on the evolution of *arbitrarily small* spatially nonhomogeneous perturbations of the ground state. The idea is to consider the unilateral source term $\hat{g}(v) = \tau v^-$ as the reference choice and the other cases are seen as its approximations. As a criterion for the comparison we choose the critical ratio D_{crit}. We will see that D_{crit} varies considerably for different choices of $\hat{g}(v)$ and that this variation is essential even in the case of very accurate approximations. Note that the strength of the unilateral source is $\tau = 0.075$ for all cases throughout this section. Now, we list the choices of $\hat{g}(v)$ we make, see also graphs in Figure 1.

(a) **Nonsmooth unilateral source, $\hat{g}(v) = \tau v^-$:** This is the reference case. The ground state of system (3) with this choice of $\hat{g}$ is zero and $\hat{g}$ is not differentiable there. Therefore, the linear analysis cannot be performed, but numerical experiments indicate that spatially nonhomogeneous perturbations as small as we can afford numerically, evolve to nonhomogeneous stationary solutions for the ratio of diffusions below 0.71. Note that this value is greater than the critical ratio of diffusion for the classical case ($\hat{g} \equiv 0$), which is 0.53. See Section 4 for more details.

(b) **Smooth quadratic approximation:** The nonsmooth function from the previous case can be smoothed for example as

$$\hat{g}(v) = \begin{cases} \tau(v-\varepsilon)^2/(4\varepsilon) & \text{for } |v| < \varepsilon, \\ \tau v^- & \text{for } |v| \geq \varepsilon, \end{cases} \tag{9}$$

where $\varepsilon > 0$ is a small parameter. System (3) with (2) and this choice of $\hat{g}(v)$ has a nonzero ground state depending on ε. Nevertheless, the corresponding critical ratio of diffusions can be expressed from (8). It depends on ε as well and its value in the limit $\varepsilon \to 0$ is $D_{\text{crit}}^{(b)} \approx 0.63$.

(c) **Smooth cubic approximation:** Another option how to smooth the function from the case (a) is

$$\hat{g}(v) = \begin{cases} \tau v^2(v+2\varepsilon)/\varepsilon^2 & \text{for } |v| < \varepsilon, \\ \tau v^- & \text{for } |v| \geq \varepsilon, \end{cases} \tag{10}$$

where $\varepsilon > 0$ is again a small parameter. The ground state in this case is zero and since the derivative of $\hat{g}$ at zero vanishes, the critical ratio of diffusions is the same as in the classical system, where $\hat{g} \equiv 0$. Using (8) we obtain $D_{\text{crit}}^{(c)} \approx 0.53$.

(d) **Linear cut:** The choice (a) can be approximated by a continuous piece-wise linear function such that it is smooth at the ground state. A straight-forward choice is

$$\hat{g}(v) = \begin{cases} \tau(\varepsilon-v)/2 & \text{for } |v| < \varepsilon, \\ \tau v^- & \text{for } |v| \geq \varepsilon. \end{cases} \tag{11}$$

The ground state is again shifted away from zero and its value depends on $\varepsilon > 0$. Consequently, the critical ratio of diffusions depends on ε as well. As ε decreases towards zero, it slowly decreases towards the limit value $D_{\text{crit}}^{(d)} \approx 0.60$.

(e) **Shift of the threshold to the left, $\hat{g}(v) = \tau(v+\varepsilon)^-$:** The corresponding ground state is zero for all $\varepsilon > 0$ and this $\hat{g}$ is smooth at zero. Thus, formula (8) can be easily used to obtain the same critical ratio of diffusions as in the case (c) and as in the classical case $\hat{g} \equiv 0$, i.e. $D_{\text{crit}}^{(e)} = D_{\text{crit}}^{(a)} \approx 0.53$.

(f) **Shift of the threshold to the right, $\hat{g}(v) = \tau(v-\varepsilon)^-$:** This choice yields a nonzero ground state depending on ε. The critical ratio of diffusions can be obtained from (8) and its limit for $\varepsilon \to 0$ is $D_{\text{crit}}^{(f)} \approx 0.71$.

To compare choices (a)–(f), we summarize the dependence of the critical ratio of diffusions on ε in Figure 2. Note that the accuracy of approximations (b)–(f) of the reference choice (a) is controlled by ε. Smaller ε corresponds to more accurate approximations. We clearly observe that different choices of $\hat{g}(v)$ yield considerably different critical ratios of diffusions and, hence, various approximations of the nonsmooth unilateral term τv^- exhibit the Turing instability for different values of the ratio D. For example, if $\varepsilon = 0.005$ and $D = 0.65$ (see the grey

(a) $\hat{g}(v) = \tau v^-$ (b) $\hat{g}(v)$ given by (9)   (c) $\hat{g}(v)$ given by (10)

(d) $\hat{g}(v)$ given by (11)   (e) $\hat{g}(v) = \tau(v + \varepsilon)^-$ (f) $\hat{g}(v) = \tau(v - \varepsilon)^-$
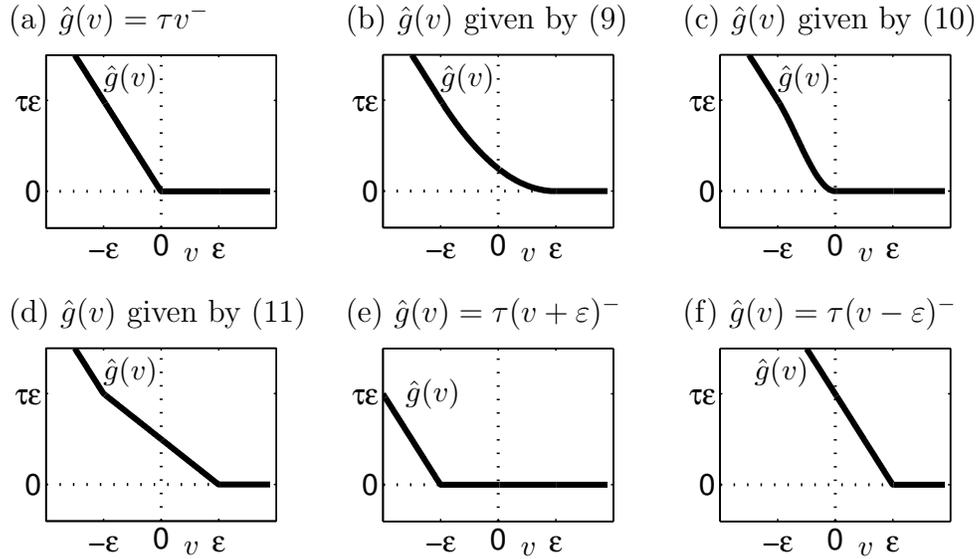

FIGURE 1.   Graphs of different choices of the unilateral term $\hat{g}(v)$ in (3).

diamond in Figure 2), then choice (a) is the only case which exhibits the Turing instability. Indeed, in cases (b)–(e) the ground state is stable with respect to all small perturbations, because the ratio of diffusion $D = 0.65$ is above the critical value and, hence, the Turing instability cannot occur. In the case (f) the Turing instability cannot occur, because tr B is positive for $\varepsilon > 0.0044$ and therefore the ground state is not stable with respect to spatially homogeneous perturbations. Similarly, if we decrease ε to 0.001 and keep $D = 0.65$, then the choices (a) and (f) exhibit the Turing instability, but choices (b)–(e) do not.

Note that our statement that the choice (a) exhibits the Turing instability is based on numerical experiments, where we observe that small perturbations of the ground state evolve to patterns. For more details and numerical results, see Figure 5 below, the panels for $\tau = 0.075$.

Figure 2 clearly shows the size of variations in D_{crit} for different approximations of the nonsmooth unilateral source term. Even if we arbitrarily increase the accuracy of these approximations, i.e. in the limit $\varepsilon \to 0$, the corresponding values of D_{crit} differ considerably. Hence, various approximations yield the Turing instability for various values of the ratio of diffusions D. Consequently, the idea to approximate the nonsmooth term by a smooth one and analyse it by standard means fails. Simple smooth approximations of the nonsmooth unilateral term with accuracy controlled by ε can yield misleading results in the limit $\varepsilon \to 0$.

From the biological perspective, all choices (a)–(f) seem to be plausible. Although some of these choices have the threshold value shifted from the ground state, the difference is not large, and, thus, they correspond to the biological motivation discussed in Section 2. However, the idea that the concentrations of
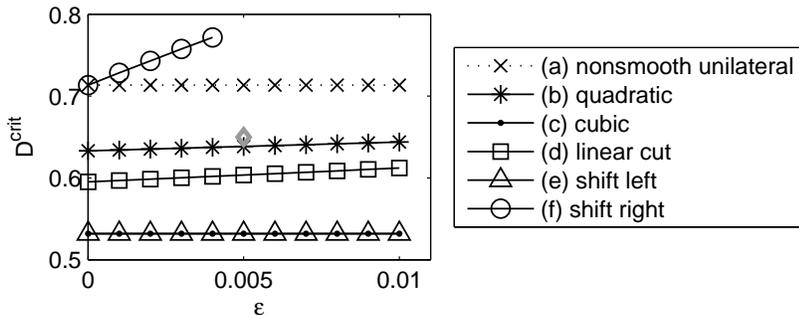
FIGURE 2.   Dependence of the critical ratio of diffusions D_{crit} on ε for choices (a)–(f). The value for choice (a) is estimated numerically and the other values are computed by (8). The grey diamond indicates parameter values ($\varepsilon = 0.005$ and $D = 0.65$) for which Turing patterns appear in the case (a) only.

morphogens grow from zero during the ontogeny favour the choice (e), where the threshold value is shifted below the ground state.

Of course, we could also discuss many other approximations of the nonsmooth unilateral term. However, results of the next subsection indicate that all these approximations result to the same (or very similar) patterns as the unilateral term $\hat{g}(v) = \tau v^-$, provided the other parameters of the problem are the same. At the same time, it is important to mention that not all of these approximations yield patterns developing from arbitrarily small perturbations. Sometimes, the perturbations have to be sufficiently distant from the ground state, as we describe below.

3.2. **Shapes of patterns for various choices of $\hat{g}(v)$.** Above, we introduced an example of parameter values for system (3) such that *arbitrary small* perturbations of the ground state do not evolve to any patterns in cases (b)–(f), but they do in the case (a), see the grey diamond in Figure 2. Now, we will see that perturbations *larger* than a certain minimal size (depending on ε) do evolve to patterns in all these cases. We also show that all these patterns are qualitatively the same. Moreover, if they evolve form the same initial condition, they are all also quantitatively very similar and some of them are even exactly identical, see Figure 3.

Similarity of these patterns is not surprising, because the differences among all choices of $\hat{g}(v)$ in cases (a)–(f) are insignificant on scales considerably larger than ε. Since the magnitude of the final pattern (i.e. the stationary solution to (3)) is of order one and the size of ε is of order one thousands, we can expect similar patterns in all these cases.

As we have mentioned, arbitrarily small perturbations of the ground state do not evolve to any patterns in cases (b)–(f) for the chosen values $D = 0.65$

(a) $\hat{g}(v) = \tau v^-$ (b) $\hat{g}(v)$ given by (9)   (c) $\hat{g}(v)$ given by (10)

(d) $\hat{g}(v)$ given by (11)   (e) $\hat{g}(v) = \tau(v+\varepsilon)^-$ (f) $\hat{g}(v) = \tau(v-\varepsilon)^-$
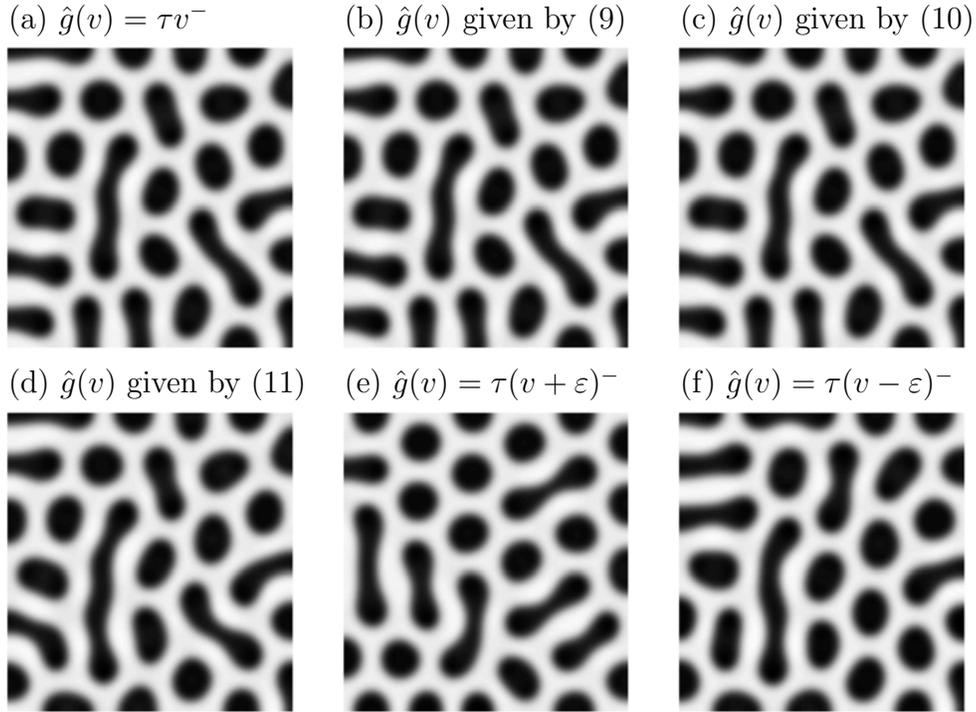

FIGURE 3.   Patterns produced from larger perturbations of the ground state in cases (a)–(f) with $D = 0.65$, $\varepsilon = 0.005$, $\tau = 0.075$, and parameter values (4). The initial condition is the same in all cases and consists of random disturbances of the ground state with maximal amplitude $20\varepsilon = 0.1$. The colour scale is identical in all cases.

and $\varepsilon = 0.005$. This fact follows from the linear analysis and we observe it numerically as well. However, Figure 3 shows that perturbations that are larger than a certain minimal size, do evolve to patterns in all these cases. Moreover, we observe identical patterns for choices (a)–(c) and a very similar pattern for the choice (d). Choices (e) and (f) yield slightly more distinct patterns, but they share the same qualitative features as the other cases.

We also computed the patterns starting from an initial condition twice as large as was used in Figure 3 and we obtained identical patterns for all cases (a)–(d). (These results are not presented.) Patterns (e) and (f) were different in a similar manner as in Figure 3. This is understandable, because choices (a)–(d) of $\hat{g}(v)$ are identical for the $|v| \geq \varepsilon$ and thus if the size of the initial condition is sufficiently large, the influence of $\hat{g}(v)$ for $|v| \geq \varepsilon$ overweights the influence of $\hat{g}(v)$ for $|v| < \varepsilon$ and identical patterns emerge. On the contrary, in cases (e) and (f) the values $\hat{g}(v)$ slightly differ even for $|v| \geq \varepsilon$ and therefore the resulting patterns differ as well. These considerations lead us to a conjecture that if two nonlinear kinetics

differ on a small neighbourhood of the ground state only, then sufficiently large initial perturbation of the ground state will evolve to the same pattern for both kinetics. If this conjecture is true then practically relevant is the evolution of perturbations greater than a certain minimal size rather than the evolution of arbitrarily small perturbations. The reason is the robustness of the evolution of the larger perturbations to patterns and the fact that the stability with respect to the arbitrarily small perturbations is highly sensitive to small changes of $\hat{g}(v)$ in the neighbourhood of the ground state.

Importantly, the nonsmooth unilateral term (a) yields patterns that evolve from arbitrarily small spatial perturbations for a large range of values of D, as far as we can conclude from numerous numerical experiments we performed. This is the essential motivation to investigate the nonsmooth unilateral case (a). It provides predictions about a whole class of approximations of the nonsmooth term $\hat{g}(v) = \tau v^-$. The tested choices (b)–(f) are just examples of members of this class. All approximations from this class produce the desired patterns and all these patterns are similar, however, for certain approximations the patterns do not evolve from arbitrarily small perturbations. There is no known theory so far that would explain the evolution of initial perturbations that are not arbitrarily small. However, the approaches presented in [9, 14, 17] provide certain ideas how to treat theoretically the positive homogeneous nonsmooth case $\hat{g}(v) = \tau v^-$. And, as we have already mentioned, the stability and instability of the ground state in systems with this term seem to correspond to the question whether the larger perturbations of the ground state do evolve to patterns or not for systems where this term is approximated.

4. Existence and shape of patterns, dependence on parameters

In this section we further investigate system (3) with the nonsmooth unilateral term $\hat{g}(v) = \tau v^-$ to show when the Turing instability occurs, what is the effect of this term on the shape of the resulting patterns, and how they depend on the strength τ and on the ratio of diffusions D. In addition, we numerically compare behaviour of this nonsmooth unilateral term with the behaviour of its linear approximations from the right and left. Namely with choices $\hat{g} \equiv 0$ (i.e. the classcial case) and $\hat{g}(v) = -\tau v$, respectively. Comparing to these linear approximations, we show that the unilateral term produces irregular patterns. Further, we present numerical results indicating that system (3) with the nonsmooth term $\hat{g}(v) = \tau v^-$ yields patterns for considerably higher ratio of diffusion constants comparing to the classical system with $\hat{g} \equiv 0$. In addition, the approximation from the left seem to be informative about the Turing instability of the nonsmooth unilateral term. For system (3), we present experiments supporting the hypothesis that the Turing instability occurs in the nonsmooth unilateral case $\hat{g}(v) = \tau v^-$ for the same ratio of diffusion coefficients as for the linear approximation from the left
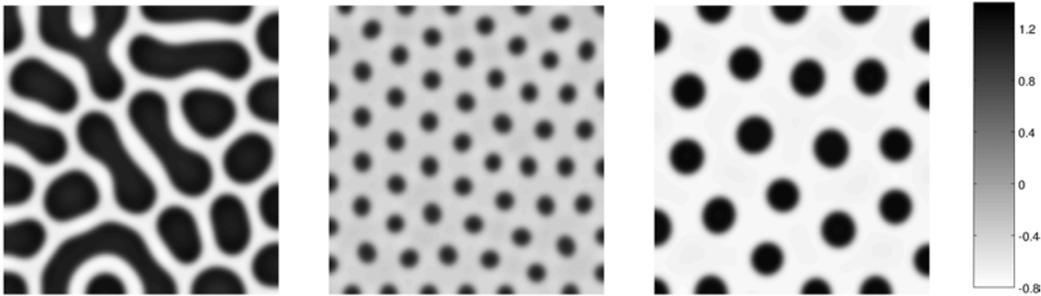
FIGURE 4.   Typical patterns obtained by system (3) with the nonsmooth unilateral term $\hat{g}(v) = \tau v^-$ (left panel), linear approximation from the right – the classical case $\hat{g} \equiv 0$ (middle panel), and linear approximation from the left $\hat{g}(v) = -\tau v$ (right panel) with $\tau = 0.08$, $D = 0.45$, and parameter values (4). The initial condition was specified as a small random noise around the ground state. The grey scale shows the values of u.

$\hat{g}(v) = -\tau v$. Finally, in the last part of this section, we compare the patterns obtained with the nonsmooth unilateral term with the coat pattern of king cheetah and suggest a mechanism generating this pattern.

4.1. **Unilateral term yields irregular patterns.** First, we compare the patterns produced by the nonsmooth unilateral term and its linear approximations from the right and left. To this end we consider system (3) with boundary conditions (2), and parameter values (4). Figure 4 compares patterns for choices $\hat{g}(v) = \tau v^-$, $\hat{g} \equiv 0$, and $\hat{g}(v) = -\tau v$, respectively, for $\tau = 0.08$ and $D = 0.45$. Comparing these patterns we immediately observe the qualitative difference. The linear choices of $\hat{g}(v)$ produce approximately circular spots which are, to some extend, symmetrically placed. In contrast, the pattern produced by the unilateral system shows irregular spots of larger size. Several of the largest spots seem to be created by fusions of smaller spots. Moreover, the pattern does not exhibit any symmetry even approximately.

4.2. **Critical ratio of diffusions.** Another interesting phenomenon resulting from the addition of the nonlinear unilateral source terms to the classical system (i.e. (3) with $\hat{g} \equiv 0$) is the growth of small nonhomogeneous perturbations of the ground state to patterns even if the ratio of diffusions exceeds the critical value (8) of the classical system (i.e. $\hat{g} \equiv 0$). Indeed, the critical ratio of diffusions (8) for the classical system with parameter values (4) is $D_{\text{crit}} \approx 0.53$. However, using the nonsmooth unilateral source $\hat{g}(v) = \tau v^-$, we numerically obtain patterns forming from very small spatial perturbations of the ground state even for considerably higher ratios of diffusions.
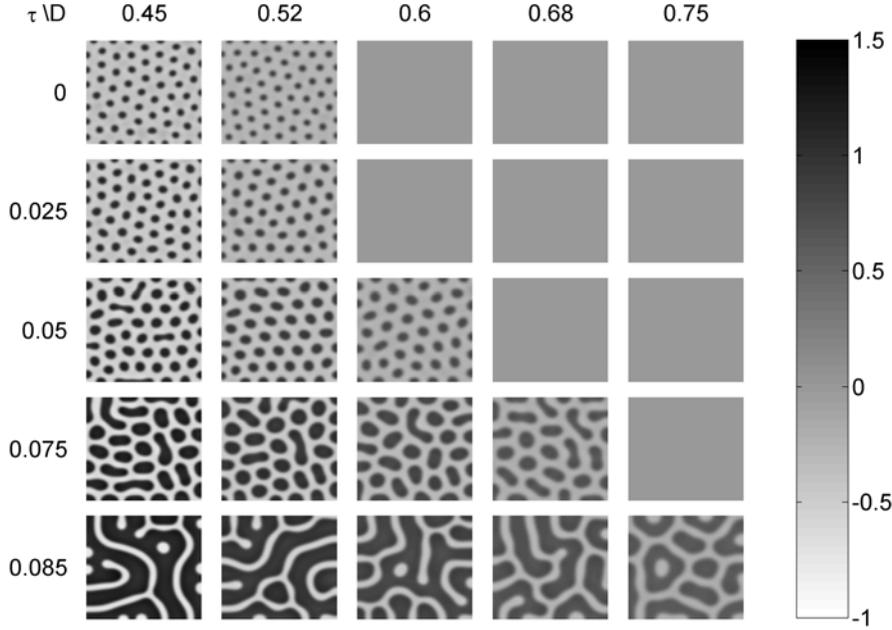
FIGURE 5.   Dependence of patterns on the ratio of diffusions D and the strength of the unilateral source τ for the nonsmooth unilateral term $\hat{g}(v) = \tau v^-$. Each box corresponds to the indicated values of D and τ and to parameter values (4).

In order to illustrate the dependence of the arising patterns on the strength of the unilateral source τ and on the ratio of diffusion constants D, we present Figure 5. The top-left box in Figure 5 corresponds to the classical system ($\hat{g} \equiv 0$) with standard parameter values (4) and $D = 0.45$. We observe the typical regular spotted pattern. As τ increases, the spots are growing bigger and starting from certain value they seem to merge and irregular patterns emerge. Similarly, we can observe that higher values of τ enable to produce patterns for higher ratios of diffusions D. In particular, columns 3–5 show that if D exceeds the critical ratio of diffusions $D_{\mathrm{crit}} \approx 0.53$ of the classical system, then the spatial patterns arise only if τ is sufficiently large. The larger is D, the larger τ is necessary for patterns to arise. For completeness, we mention that no patterns emerge for $\tau \geq 0.089$.

4.3. **Linear approximation from the left.** It is interesting to compare these results with the linear approximation of the unilateral term from the left, i.e. with the choice $\hat{g} = -\tau v$. Note that this choice can actually be seen as the classical system with $\hat{g} \equiv 0$ and coefficient β modified to $\beta - \tau$. Figure 6 shows

the resulting patterns for various values of D and τ. This system is smooth and therefore we can analyse the Turing instability including the critical ratios of diffusion coefficients (8). Table 1 presents these values for parameters (4) and various τ. Figure 6 confirms that this system produces patterns only if the ratio of diffusion coefficients is below the critical value. Interestingly, we observe patterns for the same values of the ratio of diffusions as for the system with $\hat{g} = \tau v^-$ presented in Figure 5. This leads us to a hypothesis that the Turing instability in the unilateral system (3) with $\hat{g} = \tau v^-$ occurs under the same conditions as in the case of the linear approximation (system (3) with $\hat{g} = -\tau v$). Although, we do not present the results, we solved system (3) with the nonsmooth unilateral term many times for values D close to the critical one and all these results confirmed this hypothesis.

On the other hand, comparison of Figures 5 and 6 clearly reveals the difference of the resulting patterns. The difference is even qualitative. While the patterns produced by the unilateral term are irregular with large irregular spots, patterns produced by the linear term are approximately symmetric with smaller circular spots. This qualitative difference can be explained by the substantial difference of the corresponding nonlinear dynamics especially for values of v distant from the ground state.

4.4. **King cheetah patterns.** It has been shown that *Taqpep* gene is responsible for the regularity of pre-pattern in the case of domestic cats and cheetahs [13], see Figure 7 (left). King cheetahs have a mutation in this gene and their specific coat pattern is characterized by irregular, large spots, see Figure 7 (right).

A possible explanation can be that this irregular pattern is caused by a unilateral regulation in morphogens and that the *Taqpep* gene is responsible for the strengths of the unilateral source, which we model by the coefficient τ. This leads to the hypothesis that in the common morph of cheetah the unilateral regulation is weak (τ close to zero), resulting in the usual spotted pattern, but in king cheetahs, the mutation in *Taqpep* gene can yield stronger unilateral regulation (τ around 0.08). For illustration, we may compare the model pattern in Figure 4 (middle) with the photograph of the common morph of cheetah in Figure 7 (left) and the model pattern in Figure 4 (left) with the photograph of the king cheetah in Figure 7 (right).

τ	0	0.025	0.05	0.075	0.08	0.085
D_{crit}	0.53	0.57	0.62	0.71	0.74	0.78

TABLE 1.   Critical ratios (8) of diffusion coefficients for the linear source term (i.e. system (3) with $\hat{g}(v) = -\tau v$) and various values of τ. Rounded to two significant digits.
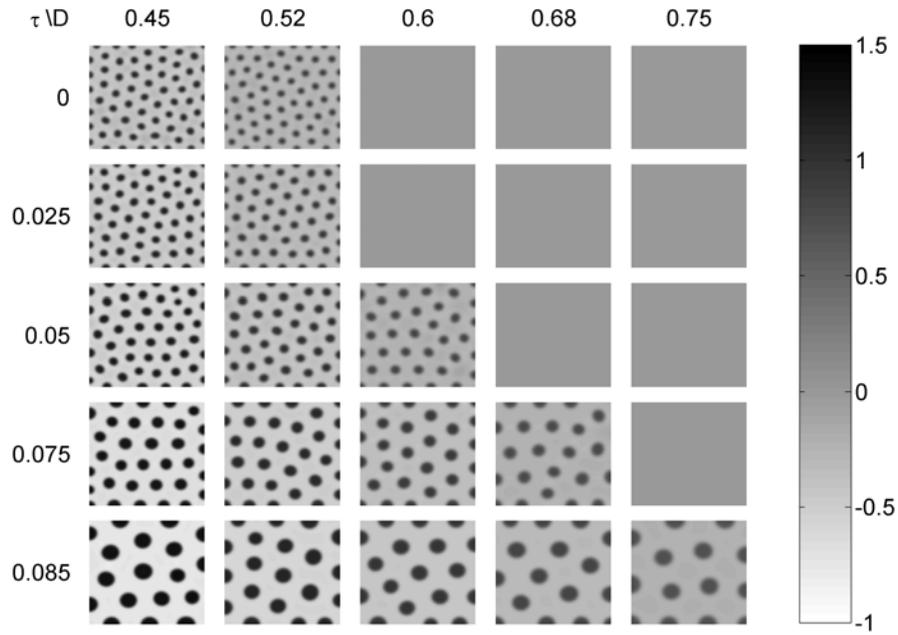
FIGURE 6.   Dependence of patterns on D and τ for the linear approximation of the unilateral term from the left, i.e. $\hat{g}(v) = -\tau v$. Each box corresponds to the indicated values of D and τ and to parameter values (4).

FIGURE 7.   Typical coat patterns of cheetah (left) and king cheetah (right).

5. Discussion and conclusions

In this contribution we investigated a reaction-diffusion system with a non-smooth unilateral source term of type $\hat{g}(v) = \tau v^-$ and its approximations. We provided a case study for a particular system and analysed numerically the influence of the nonsmooth unilateral source on the Turing instability and on the resulting patterns. We explained a possible biological meaning of this term. The standard linear analysis cannot be applied to nonsmooth systems and we demonstrated that the linear analysis of systems with smooth approximations of the term $\hat{g}(v) = \tau v^-$ is not informative about the Turing instability of the system with the nonsmooth term. Arbitrarily small perturbations of the ground state can evolve to patterns for one approximation of the nonsmooth term, but not for the other even though they are arbitrarily accurate. This shows that the Turing instability is sensitive to small changes of the nonlinear dynamics. However, we also showed that initial perturbations of the ground state larger than a certain minimal size do robustly evolve to patterns for both the nonsmooth term and its approximations. In addition, these patterns are almost identical regardless the particular form of the unilateral term in the small neighbourhood of the ground state.

We have found that unilateral sources break the approximate regularity and symmetry of the usual patterns. For example, system (3) with the unilateral term $\hat{g}(v) = \tau v^-$ produces spots with irregular shapes and variable distances between them. This contrasts to the classical smooth systems corresponding to choices $\hat{g} \equiv 0$ and $\hat{g}(v) = -\tau v$ in (3), where we observe close-to-regular disc-shaped spots approximately symmetrically placed, see Figure 4.

Interestingly, system (3) with the unilateral term $\hat{g}(v) = \tau v^-$ produces patterns even for those values of diffusion constants which prevent any pattern formation in the original system (i.e. $\hat{g} \equiv 0$). Further, we observe that the critical ratio of diffusions for the system with $\hat{g}(v) = \tau v^-$ seems to be identical to the critical ratio of the linear approximation from the left, i.e. the choice $\hat{g}(v) = -\tau v$. However, the resulting patterns differ considerably. A general conclusion of these experiments is that the unilateral sources prescribed for the inhibitor v break the regularity of patterns for all values of diffusion constants yielding patterns, provided the strength of the unilateral source is not negligible. In addition, recent experiments [23] with adding a unilateral term to the Thomas model [25] yield the same conclusions and indicate that our findings about the effects of the unilateral term are not limited to a single model.

Reaction-diffusion systems with nonsmooth unilateral terms are interesting from both the theoretical and practical points of view. In contrasts to the classical smooth case, where the small perturbations initially evolve according to a linear dynamics, the evolution of small perturbations of the ground state for the nonsmooth unilateral term is inherently governed by a nonlinear dynamics. This

nonlinear dynamics may yield completely new phenomena in the pattern formation mechanisms. In this contribution, we have made an attempt towards the understanding of the unilateral terms in models of biological patterns formation. However, further research is necessary for the investigation of feasible biological applications.

References

[1] Barrio, R., Varea, C., Aragón, J., Maini, P.: A two-dimensional numerical study of spatial pattern formation in interacting turing systems. Bulletin of mathematical biology **61**(3), 483–505 (1999)

[2] Chen, Y., Schier, A.F.: The zebrafish nodal signal squint functions as a morphogen. Nature **411**(6837), 607–610 (2001)

[3] Crampin, E., Gaffney, E., Maini, P.: Mode-doubling and tripling in reaction-diffusion patterns on growing domains: A piecewise linear model. Journal of mathematical biology **44**(2), 107–128 (2002)

[4] Crampin, E.J., Gaffney, E.A., Maini, P.K.: Reaction and diffusion on growing domains: scenarios for robust pattern formation. Bulletin of mathematical biology **61**(6), 1093–1120 (1999)

[5] Drábek, P., Kučera, M., Míková, M.: Bifurcation points of reaction-diffusion systems with unilateral conditions. Czechoslovak Mathematical Journal **35**(4), 639–660 (1985)

[6] Economou, A.D., Ohazama, A., Porntaveetus, T., Sharpe, P.T., Kondo, S., Basson, M.A., Gritli-Linde, A., Cobourne, M.T., Green, J.B.: Periodic stripe formation by a Turing mechanism operating at growth zones in the mammalian palate. Nature genetics **44**(3), 348–351 (2012)

[7] Edelstein-Keshet, L.: Mathematical models in biology. McGraw-Hill, Boston (1988)

[8] Eisner, J., Kučera, M.: Spatial patterning in reaction-diffusion systems with nonstandard boundary conditions. Fields Inst. Commun. **25**, 239–256 (2000)

[9] Eisner, J., Kučera, M.: Bifurcation of solutions to reaction-diffusion systems with jumping nonlinearities. In: A. Sequeira, H. Beirao da Veiga, J.H. Videman (eds.) Applied Nonlinear Analysis, pp. 79–96. Springer (2002)

[10] Eisner, J., Väth, M.: Location of bifurcation points for a reaction-diffusion system with Neumann-Signorini conditions. Advanced Nonlinear Studies **11**(4), 809–836 (2011)

[11] Hannezo, E., Prost, J., Joanny, J.F.: Growth, homeostatic regulation and stem cell dynamics in tissues. Journal of The Royal Society Interface **11**(93), 20130895 (2014)

[12] Jones, D.S., Sleeman, B.D.: Differential Equations and Mathematical Biology. Chapman & Hall (2003)

[13] Kaelin, C.B., Xu, X., Hong, L.Z., David, V.A., McGowan, K.A., Schmidt-Küntzel, A., Roelke, M.E., Pino, J., Pontius, J., Cooper, G.M., et al.: Specifying and sustaining pigmentation patterns in domestic and wild cats. Science **337**(6101), 1536–1541 (2012)

[14] Kim, I.S., Väth, M.: The Krasnoselskii-Quittner formula and instability of a reaction-diffusion system with unilateral obstacles. Dynamics of Partial Differential Equations **11**(3), 229–250 (2014)

[15] Kondo, S.: The reaction-diffusion system: a mechanism for autonomous pattern formation in the animal skin. Genes to Cells **7**(6), 535–541 (2002)

[16] Kondo, S., Miura, T.: Reaction-diffusion model as a framework for understanding biological pattern formation. Science **329**(5999), 1616–1620 (2010)

[17] Kučera, M., Väth, M.: Bifurcation for a reaction–diffusion system with unilateral and Neumann boundary conditions. Journal of Differential Equations **252**(4), 2951–2982 (2012)

[18] Kučera, M., Bosák, M.: Bifurcation for quasi-variational inequalities of reaction-diffusion type. Stability and Applied Analysis of Continuous Media **3**(2), 354–369 (1994)

[19] Liu, R., Liaw, S., Maini, P.: Two-stage Turing model for generating pigment patterns on the leopard and the jaguar. Physical review E **74**(1), 011914 (2006)

[20] Mou, C., Jackson, B., Schneider, P., Overbeek, P.A., Headon, D.J.: Generation of the primary hair follicle pattern. Proceedings of the National Academy of Sciences **103**(24), 9075–9080 (2006)

[21] Murray, J.D.: Mathematical biology. II. Spatial models and biomedical applications. Springer-Verlag (2003)

[22] Nishiura, Y.: Global structure of bifurcating solutions of some reaction-diffusion systems. SIAM Journal on Mathematical Analysis **13**(4), 555–593 (1982)

[23] Rybář, V., Vejchodský, T.: Irregularity of Turing patterns in the Thomas model with a unilateral term. In: J. Chleboun, P. Přikryl, K. Segeth, J. Šístek, T. Vejchodský (eds.) Programs and Algorithms of Numerical Matematics 17. Institute of Mathematics AS CR (2015). To appear.

[24] Schier, A.F.: Nodal morphogens. Cold Spring Harbor perspectives in biology **1**(5), a003459 (2009)

[25] Thomas, D.: Artificial enzyme membranes, transport, memory, and oscillatory phenomena. In: D. Thomas, J.P. Kernevez (eds.) Analysis and control of immobilized enzyme systems, pp. 115–150. North Holland (1976)

[26] Turing, A.M.: The chemical basis of morphogenesis. Philosophical Transactions of the Royal Society of London B: Biological Sciences **237**(641), 37–72 (1952)

[27] Varea, C., Aragón, J., Barrio, R.: Confined Turing patterns in growing systems. Physical Review E **56**(1), 1250–1253 (1997)

TOMÁŠ VEJCHODSKÝ, INSTITUTE OF MATHEMATICS, ACADEMY OF SCIENCES, ŽITNÁ 25, CZ-115 67 PRAHA 1, CZECH REPUBLIC,
  E-mail address: vejchod@math.cas.cz

FILIP JAROŠ, FACULTY OF ARTS, UNIVERSITY OF HRADEC KRÁLOVÉ, NÁMĚSTÍ SVOBODY 331, CZ-500 02 HRADEC KRÁLOVÉ, CZECH REPUBLIC.
  E-mail address: filip.jaros@uhk.cz

MILAN KUČERA, INSTITUTE OF MATHEMATICS, ACADEMY OF SCIENCES, ŽITNÁ 25, CZ-115 67 PRAHA 1, CZECH REPUBLIC AND DEPARTMENT OF MATHEMATICS, FACULTY OF APPLIED SCIENCES, UNIVERSITY OF WEST BOHEMIA IN PILSEN, UNIVERZITNÍ 8, 30614 PLZEŇ, CZECH REPUBLIC.
  E-mail address: kucera@math.cas.cz

VOJTĚCH RYBÁŘ, INSTITUTE OF MATHEMATICS, ACADEMY OF SCIENCES, ŽITNÁ 25, CZ-115 67 PRAHA 1, CZECH REPUBLIC.
  E-mail address: rybar@math.cas.cz